

Tuesday, July 28, 1998
PRESOLAR GRAINS AND ISOTOPIC ANOMALIES II
1:30 p.m. Walton Theatre

Chairs: L. R. Nittler
P. Hoppe

- Koscheev A. P.* Gromov M. D. Herrmann S. Ott U.
Mass Fractionation and Thermal Release from Nanodiamonds of Low-Energy Implanted Xenon
- Braatz A.* Dorschner J. Henning Th. Jäger C. Ott U.
Infrared Spectra of Presolar Diamonds: The Influence of Chemical Preparation
- Banhart F. Lyutovich Y. Braatz A. Jäger C. Henning T. Dorschner J. Ott U.*
Presolar Diamond in Unprocessed Allende
- Huss G. R.* Meshik A. Kehm K. Hohenberg C.
Presolar Diamonds in Roosevelt County 075 and Axtell: Abundances and Noble Gas Characteristics
- Meshik A. P.* Pravdivtseva O. V. Hohenberg C. M.
Selective Laser Extraction of Gases from Mineral Populations with Different Optical Properties: A First Test on Murchison Diamonds
- Verchovsky A. B.* Gilmour J. D. Fisenko A. V. Semjonova L. F. Wright I. P. Turner G. Pillinger C. T.
Isotopic Analyses of Xenon in Grain-sized Fractions of Presolar Diamonds from Efremovka Using RELAX
- Daulton T. L.* Lewis R. S. Amari S.
Polytype Variations in Presolar Silicon Carbide Grains: Microstructural Characterization by Transmission Electron Microscopy
- Nittler L. R.* Alexander C. M. O'D.
Automated Isotopic Measurements of Presolar Grains
- Swan P. D. Walker R. M.*
Distribution of In Situ Silicon Carbide Grains in Primitive Meteorites and Their Use in Identifying Nebular Components
- Gallino R.* Travaglio C. Zinner E. Amari S. Woosley S.
Predicted Strontium-, Zirconium-, and Molybdenum-Isotopic Composition in Presolar Grains from Type II SNe
- Travaglio C.* Gallino R. Zinner E. Amari S. Woosley S.
Presolar Grains from SN Type II: The Case of Silicon- and Calcium-Isotopic Composition
- Nicolussi G. K.* Pellin M. J. Lewis R. S. Davis A. M. Clayton R. N. Amari S.
Strontium Isotopes in Single Presolar Silicon Carbide Grains
- Hoppe P.* Kocher Th. Eberhardt P. Amari S. Lewis R. S.
Carbon- and Nitrogen-Isotopic Compositions of Individual, Submicrometer-sized Presolar Silicon Carbide Grains
- Rooke G. P.* Franchi I. A. Verchovsky A. B. Pillinger C. T.
Nitrogen-15-rich Nitrogen in Meteorites: Polymict Ureilites and Bencubbin
- Hill H. G. M.* Jones A. P. d'Hendecourt L. B.
The "21-Micrometer" Infrared Feature in Bulk Diamonds: Implications for Nanodiamonds in Space

MASS FRACTIONATION AND THERMAL RELEASE FROM NANODIAMONDS OF LOW-ENERGY IMPLANTED XENON. A. P. Koscheev¹, M. D. Gromov¹, S. Herrmann², and U. Ott². ¹Karpov Institute of Physical Chemistry, ul. Vorontzovo Pole 10, Moscow, 103064, Russia, ²Max-Planck-Institut für Chemie, Becherweg 27, D-55128 Mainz, Germany (ott@mpch-mainz.mpg.de).

Ion implantation has been explored by various authors [1,2; and references therein] as a general way of introducing “trapped” noble gases into matter. We report studies along these lines, using a phase of definite cosmochemical relevance: nanodiamonds similar to those that have been shown to contain, among others, isotopically exotic xenon (Xe-HL) [3].

The nanodiamonds used were “ultradispersed” (UDD) diamonds produced by detonation processes in the Russian Federal Centre - Research Institute of Technical Physics - with a size estimated as approx. 3 nm. Xe ions were implanted using a modified ionization gauge, with a colloid of UDD diamonds deposited on the collector. The results reported here were obtained for ion energies of 250 eV (dose: $3 \times 10^{15} \text{ cm}^{-2}$) followed by heating to 550°C and a second implantation with a dose of $9 \times 10^{14} \text{ cm}^{-2}$ and 1200 eV (dose: $2 \times 10^{16} \text{ cm}^{-2}$).

The gas release pattern is similar to that of the isotopically non-spectacular Xe-P3 component in meteoritic nanodiamonds [4,5]. Apparent diffusion constants have been calculated as in [5] and plotted in an Arrhenius plot (see Fig. 1). While values for Murchison and artificial nanodiamonds are similar, there is a slight difference in slope corresponding to somewhat different activation energies. As noted in [5], the release data can also be described by a “chemical erosion” model.

Relative to the starting composition, the trapped Xe is mass fractionated, favoring the heavy isotopes by, overall, approx. 0.5 %/amu, similar to the results of [1,2], supporting the general validity of the descriptions of the trapping process given there. In addition, variations were observed between the different temperature steps, the fractionation increasing from ca. 0.3%/amu at the lowest temperature to as much as 1.5% at the highest release temperature. It seems noteworthy that relative to solar wind xenon [6] Xe-P3 shows a similar fractionation relationship with the heavy isotopes relatively enriched by about 1%/amu (isotopes 129 and 130 slightly deviate from the trend). This observation may suggest an intrinsic relationship between the P3 component in presolar meteorites and solar type noble gases.

The similar release of low-energy ion implanted Xe and of the Xe-P3 component in presolar diamond suggests a similar siting within the carrier nanodiamonds. Based on its relatively low release temperature, Xe-P3 has often been interpreted as a surface-correlated component [4], but, since the range of the low-energy ions used in our experiment is on the order of the size of the nanodiamonds (cf. [2]), our simulation data do not support this. Rather, they suggest that Xe-P3 and Xe-HL, which is released at higher temperature, may reside in two basically different types of carriers. Nevertheless, whatever the Xe-HL carrier, it must resemble the nanodiamonds in its chemical properties.

Acknowledgments: This work was supported by RFBR-DFG (Grant# 96-05-00038).

References: [1] Bernatowicz T. J. and Hagee B. E. (1986) *GCA*, 51, 1599. [2] Ponganis K. V. et al. (1997) *JGR*, 102, 19335. [3] Lewis R. S. et al. (1987) *Nature*, 326, 160. [4] Huss G. R. and Lewis R. S. (1994) *Meteoritics*, 29, 791. [5] Zadnik, M. G. and Ott U. (1998) *Meteoritics and Planet. Sci.*, this issue. [6] Pepin R. O. et al. (1995) *GCA*, 59, 4997.

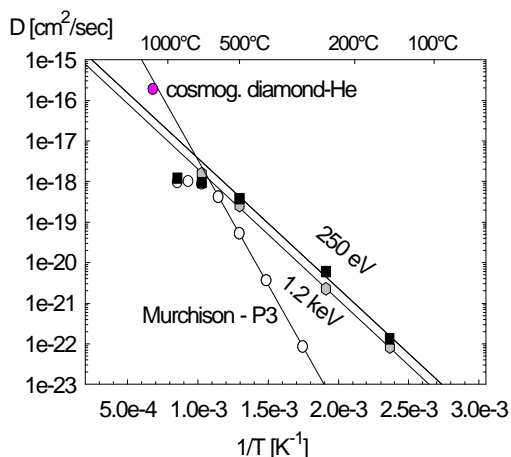


Fig. 1.

In the infrared region, chemically pure diamonds without structural defects display only one broad absorption band between 2700 and 1660 cm^{-1} [1]. All other absorption bands are caused by structural defects or chemical contamination within and on the surface of the diamonds. The infrared spectra of presolar diamonds isolated from primitive meteorites display many absorptions bands [2-5]. The problem is to determine the origin of these bands and whether they are intrinsic to the presolar diamonds or of secondary origin. In order to address this question, we prepared diamond residues (in general following [6]) from the Murchison and Allende meteorites, with infrared spectra taken and chemical analyses (by SEM/EDX) performed after each step of the preparation procedure.

The infrared spectra of our cleanest diamond fractions show absorption bands at: 3670-3070 cm^{-1} , 3000-2800 cm^{-1} , 1860-1560 cm^{-1} , 1400-790 cm^{-1} , 660-480 cm^{-1} , and 120 cm^{-1} . The corresponding functional groups are $-\text{OH}$ for the absorption at 3670-3070 cm^{-1} and 1620 cm^{-1} , $-\text{CH}_2$ and $-\text{CH}_3$ for 3000-2800 cm^{-1} , and $\text{C}=\text{O}$ for 1700 cm^{-1} . The absorption between 660-490 cm^{-1} is due to residual spinel grains. It is still unknown which functional group generates the absorption band at 120 cm^{-1} . Many functional groups absorb between 1400 and 790 cm^{-1} , but based on the measurements of [7] and our own chemical analyses, C-N-C, C-O-C, $-\text{CF}$ and $-\text{CF}_2$ are the most viable candidates.

The issue then is to determine the origin of the functional groups:

$-\text{CH}_2$, $-\text{CH}_3$: Because of their structure these groups appear on the diamond surface. Occurrence and strength of their absorption vary strongly, even in spectra of the same sample. Mutschke et al. [4] concluded that they "come from terrestrial adsorbed hydrocarbons rather than from originally present CH groups of interstellar origin".

$\text{C}=\text{O}$, C-O-C, $-\text{COOH}$: The $\text{C}=\text{O}/-\text{COOH}$ groups can only exist on the diamond surface, too. During the preparation the strength of the $\text{C}=\text{O}$ peak at 1700 cm^{-1} increases compared to other peaks, e.g. the $-\text{OH}$ peak at 1620 cm^{-1} .

This indicates an increasing oxidation of the sample during the preparation, due to the use of oxidizing chemicals. The resulting $\text{C}=\text{O}$ -, C-O-C- and $-\text{COOH}$ groups are most probably artifacts.

$-\text{OH}$: One source of $-\text{OH}$ groups could be KBr, the carrier of our diamond samples during the spectroscopic measurements [4]. In addition, because of their oxidized surfaces, the diamonds are hydrophilic and can attract water [8].

$-\text{CF}$, $-\text{CF}_2$: These groups developed during the treatment of the sample with hot concentrated sulphuric acid in teflon containers. The acid did not only dissolve spinel grains but also attack the walls of the container.

C-N-C: Based on the results presented in [7], the presolar diamonds contain up to 1% nitrogen. The absorption peak of this group (at 1282 cm^{-1} and/or 1130 cm^{-1}) is most probably an intrinsic feature of the diamonds. Unfortunately the absorption of the $-\text{CF}$, $-\text{CF}_2$ and C-O-C groups are superimposed on this feature. Therefore, it is difficult to say, if any of the absorption bands between 1400 and 790 cm^{-1} are caused by C-N-C.

As a result, we come to the conclusion that while we cannot exclude a partially intrinsic origin of the infrared absorption features we measured, most of them are of secondary origin.

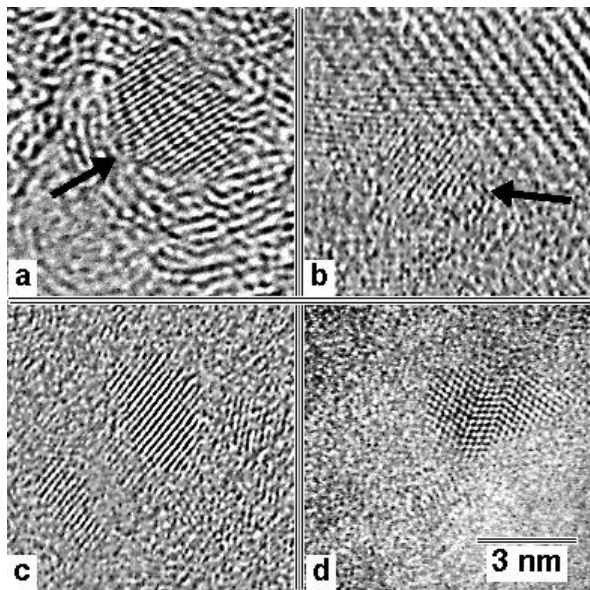
We did not find an absorption band which can unambiguously be considered a true presolar diamond feature. We could not confirm the candidate features 120 cm^{-1} [4] and 475 cm^{-1} [3]. Half of our spectra did not show the first, while the second one was not found in our spectra at all.

References:[1] Ramdas A.K. (1994) in *Properties and growth of diamond*, (G. Davies ed.), pp13-22. [2] Andersen A.C. et al. (1998) *Astron. Astrophys.*, submitted [3] Hill H.G.M. et al. (1997) *Meteoritics*, 32, 713-718. [4] Mutschke H. et al. (1995) *Astrophys.J.Lett.*, 454, L157-160. [5] Lewis R.S. et al. (1989) *Nature*, 339, 117-121. [6] Amari S. et al. (1994) *GCA*, 58, 459-470. [7] Russell S.S. et al. (1991) *Science*, 254, 1188-1191. [8] Sappok R. and Boehm H.P. (1968) *Carbon*, 6, 573-588.

PRESOLAR DIAMOND IN UNPROCESSED ALLENDE. F. Banhart¹, Y. Lyutovich¹, A. Braatz^{2,3}, C. Jäger², T. Henning², J. Dorschner², and U. Ott³, ¹Max-Planck-Institut für Metallforschung, D-70569 Stuttgart, Germany, ²Astrophysikalisches Institut, Universität Jena, D-07745 Jena, Germany; ³Max-Planck-Institut für Chemie, Becherweg 27, D-55128 Mainz, Germany (ott @mpch-mainz.mpg.de).

A type of information that is usually lost in the study of presolar phases in primitive meteorites is their actual location within the meteorites. This is because during isolation for analysis essentially all other phases are dissolved away by acids [1]. Trying to improve the situation we set out to search for the most abundant of those phases, diamond, within untreated carbonaceous chondrites. The task is not trivial, because not only is the concentration ~1 % at best, but, more importantly, the average size of these "nanodiamonds" is only about 2 nm [2].

In our search we used the Stuttgart ultra-high resolution transmission electron microscope (Jeol ARM 1250) with a present point resolution of 0.12 nm [3]. An untreated sample from Allende was crushed and the powder placed on a standard grid for electron microscopy. Large areas of meteorite matrix were scanned and checked for the occurrence of diamonds. Images and, if possible, electron energy loss spectra (EELS) were taken from suspected nanodiamond grains within their environment.



The figure shows two diamond grains found in our search, one in (a) a carbonaceous, the other in (b) a crystalline silicate environment. For comparison two grains from a chemically prepared diamond residue from Murchison [4] are shown (c,d). The identification is based on the following criteria:

- the lattice spacings of (111) and (022) planes of cubic diamond
- the typical size and shape of nanodiamond grains
- the high resistance of diamond to electron irradiation
- in some cases, EEL spectra from the grains (plus environment), showing the core-loss edge of carbon.

Important preliminary observations are as follows:

1. Most diamond grains appear single.
2. No clear preference for a certain mineralogical environment is evident. Diamond grains appear within the silicate matrix as well as within carbon-rich areas, where their abundance may be somewhat higher.
3. There is no evidence for a morphological difference between processed and unprocessed diamonds.

What is regarded as evidence for (part of) the nanodiamonds to be presolar is the presence within diamond samples of isotopically exotic Xenon-HL, but what fraction of nanodiamonds in primitive meteorites is truly presolar is not known. Since only about one in a million diamonds contains an atom of Xe, the likelihood to encounter a grain of proven interstellar origin during TEM observation of single grains is virtually zero. Nevertheless, our preliminary study suggests that the distribution of diamonds within primitive meteorites is essentially uniform and not restricted to a certain environment. Most likely, the diamonds existed prior to formation of meteoritic material into which they were mixed prior to meteorite compaction. This is to be expected if the diamonds are presolar. In that sense our observations attest to their presolar nature - but not necessarily to a circumstellar origin, which can be inferred from isotopic structures only.

References: [1] Amari S. et al. (1994) *GCA*, 58, 459. [2] Daulton T. R. et al. (1996) *GCA*, 60, 4853. [3] Phillipp F. et al. (1994) *Ultramicroscopy*, 56, 1. [4] Braatz A. (1998) Ph.D. Thesis, Universität Jena, in preparation.

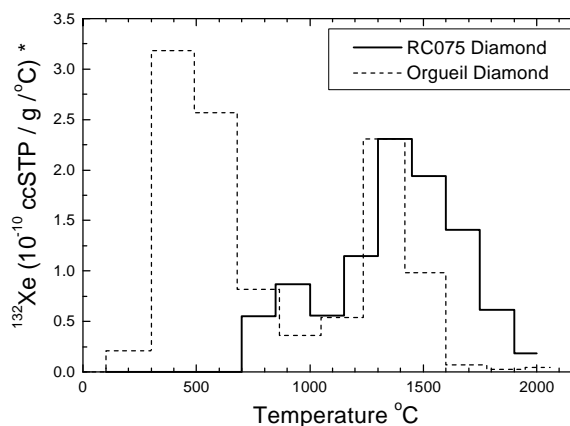
PRESOLAR DIAMONDS IN RC075 AND AXTELL: ABUNDANCES AND NOBLE GAS CHARACTERISTICS. G. R. Huss¹, A. Meshik², K. Kehm², and C. Hohenberg², ¹Lunatic Asylum, Division of Geological and Planetary Sciences, Mail Stop 170-25, California Institute of Technology, Pasadena, CA 91125 (ghuss@gps.caltech.edu), ²Department of Physics, Washington University, St. Louis, MO 63130

Presolar diamonds occur in all classes of chondrites, and their abundances and noble-gas characteristics carry a record of metamorphic heating on meteorite parent bodies [e.g., 1]. The abundance of P3 noble gases in diamonds is very sensitive to thermal history and seems to record the maximum temperature experienced by the diamonds [2]. Large differences in P3 abundance in diamonds from the *least metamorphosed* LL, EH, and CV chondrites led [2] to suggest that diamonds in these meteorites might retain a record of their nebular thermal history, but the database has been too small to fully evaluate this idea. We have begun a study of abundances and noble-gas characteristics of presolar diamonds in meteorites that fill gaps in the database. Diamond separates and etched acid residues were prepared for RC075 (H3.2), the least metamorphosed H chondrite [3], and for Axtell, an oxidized CV3 chondrite similar to Allende [4]. We report here preliminary diamond abundances for RC075 and Axtell and noble-gas data for the RC075 diamond separate.

Our preliminary diamond abundances come from yields of diamond separates, in which we typically recover ~70% of the diamonds in the meteorite [1]. These data can be compared with yields of diamond separates from other meteorites produced by the same technique. For RC075, the amount of recovered diamond (82.6 ± 1.0 ppm) is somewhat lower than those for Krymka (LL3.1; ~95 ppm) and Bishunpur (LL3.1; ~115 ppm), but is higher than those for Ragland (LL3.5; ~70 ppm) and Mezö Madaras (L3.5) or ALHA77214 (L3.5) (~52 ppm) [cf 1]. The diamond abundance for RC075 is thus consistent with a petrologic type ~3.2 [3]. For Axtell, the recovered diamond abundance (238 ± 15 ppm) is almost identical with that of Allende (~250 ppm), but is lower than those of reduced CV3's, Leoville (CV3.0 [5]; ~496 ppm [1]) and Vigarano (CV3.3 [5]; ~281 ppm [1]). Allende diamonds contain very little P3 gas, which indicates that they have been heated to ~600°C sometime in their history [2]. A metamorphic grade of ~3.2, estimated from TL sensitivity [5], implies a much lower metamorphic temperature. Perhaps the low P3 abundance in Allende diamonds and the relatively low diamond abundances in Allende and Axtell reflect the pre-

accretionary processing that produced oxidized CV3 chondrites.

Diamonds from RC075 carry the same noble gas components, as do diamonds from other chondrites (P3, HL, and P6 [6]). The ¹³²Xe release as a function of temperature for RC075 diamonds is compared to that for Orgueil diamonds in the Figure. Orgueil diamonds have a large low-temperature ¹³²Xe-P3 release peak, but the P3 release is much smaller and shifted to higher temperature in diamonds from RC075 (Figure). This indicates that RC075 diamonds have been heated to substantially higher temperature than Orgueil diamonds and have lost P3 gases. The RC075 release pattern most closely resembles that of Bishunpur (LL3.1) diamonds, which were apparently heated to ~300°C [2]. This again implies that RC075 is petrologic type ~3.2 [3].



* Orgueil data normalized to 1450 °C step in RC075.

References: [1] Huss G. R. and Lewis R. S. (1995) *GCA*, 59, 115–160. [2] Huss G. R. and Lewis R. S. (1994) *Meteoritics*, 29, 811–829. [3] McCoy T. J. et al. (1993) *Meteoritics*, 28, 681–691. [4] Simon S. B. et al. (1995) *Meteoritics*, 30, 42–46. [5] Symes S. J. K. et al. (1993) *Meteoritics*, 28, 446. [6] Huss G. R. and Lewis R. S. (1994) *Meteoritics*, 29, 791–810.

Supported by NASA NAG5-4203 to G. J. Wasserburg and NAG5-4173 to C. Hohenberg. Div. Contrib. No. 8520(1001).

SELECTIVE LASER EXTRACTION OF GASES FROM MINERAL POPULATIONS WITH DIFFERENT OPTICAL PROPERTIES: A FIRST TEST ON MURCHISON DIAMONDS A. P. Meshik, O. V. Pravdivtseva, and C. M. Hohenberg, McDonnell Center for Space Sciences, Washington University, Saint Louis MO 63130, USA (am@howdy.wustl.edu).

Introduction: We are currently exploring a new experimental method for selective noble gas extraction that is based on the differential absorption of laser light by mineral grains with different optical transparencies. This technique has been applied to the study of meteoritic nanodiamonds whose bulk optical properties are due to nitrogen impurities present in a subset of diamond grains [1]. Ideally, laser light can selectively heat high-N diamonds, preferentially extracting gases from this sub-population only. This may provide a means to decouple and measure various elemental and isotopic components such as Xe-H and Xe-L, for example, which presumably formed by different processes [2], but are heretofore inseparable.

Experiment: A colloidal solution of separated Murchison nanodiamond was prepared for this study using traditional demineralization technique [3]. Three samples were prepared, each using a 2.0 μl drop of the colloid containing $\sim 19.3 \mu\text{g}$ of diamonds. Sample A was deposited onto a piece of Pt foil for heating in a conventional resistive oven. Samples B and C were deposited over different areas on the surfaces of optically transparent $10 \times 7 \times 0.5 \text{ mm}$ sapphire plates to achieve different surface densities of diamonds. The more concentrated sample B contained ~ 2500 layers of diamond grains, while sample C was distributed over a broader area consisting of roughly a single diamond layer. Xe from the sample A was used as a reference. A defocused IR laser extracted gases from diamonds on samples B and C.

Results and Discussion: Only small differences in the Xe amount and composition were observed between sample A (degassed in the oven) and B (laser extraction). However, for sample C where diamonds were deposited in a much small surface concentration, only about 1% of total Xe was released by laser heating. Evidently complete Xe extraction from sample B was caused by the nearly isothermal conditions resulting from a high local concentration of diamonds. Thermal conductivity was not a factor for sample C where the small amount of extracted Xe may be from the high-N diamond population. Subtle isotopic differences are also observed in Xe from sample C, with Xe-L seeming somewhat suppressed compared to Xe from sample B (Fig. 1).

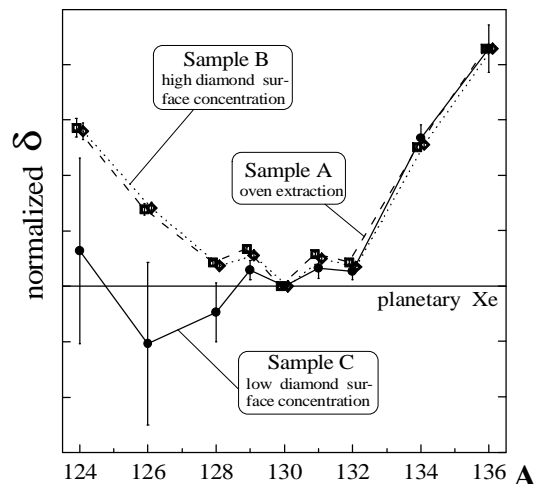


Fig. 1. Comparison of Xe released from high (~ 2500 layers) and low (\sim monolayer) diamond surface areas, normalized to ^{136}Xe .

$$d = \left[\left(\frac{A \text{ Xe}}{^{130} \text{Xe}} \right) / \left(\frac{A \text{ Xe}}{^{130} \text{Xe}} \right)_{\text{ref.}} - 1 \right] / \left[\left(\frac{^{136} \text{Xe}}{^{130} \text{Xe}} \right) / \left(\frac{^{136} \text{Xe}}{^{130} \text{Xe}} \right)_{\text{ref.}} - 1 \right]$$

Conclusion: Whether or not this proposed method is capable of separating Xe-HL, it certainly has many attractive features. For example, it is capable of releasing carbon from single or few nanodiamonds. It also possesses the minimal possible blank, since the laser heats only the absorber. We are currently in the process of installing combustion capability into the laser extraction cell. This combination might increase the selectivity of the proposed technique.

Acknowledgments: This work is supported by NASA grant NAG5-4173.

References: [1] Russel S. S. et al. (1991) *Science*, 254, 1188–1191. [2] Anders E. and Zinner E. (1993) *Meteoritics*, 28, 490–514. [3] Amari S. et al. (1994) *GCA*, 58, 459–470.

ISOTOPIC ANALYSES OF Xe IN GRAIN SIZE FRACTIONS OF PRESOLAR DIAMONDS FROM EFREMOVKA USING RELAX. A. B. Verchovsky¹, J. D. Gilmour², A.V. Fisenko³, L. F. Semjonova³ I.P Wright¹, G. Turner² and C. T. Pillinger¹; ¹Planetary Sciences Research Institute, The Open University, Milton, Keynes, United Kingdom; ²Department of Earth Sciences, Manchester University, Manchester, United Kingdom; ³Vernadsky Institute of Geochemistry and Analytical Chemistry, Russian Academy of Sciences, Moscow, Russia.

We have recently reported the first isotope analyses of N, C and noble gases in four grain size fractions of Efremovka presolar diamonds separated by ultracentrifugation (ED2, ED3, ED4, and ED9) [1]. They exhibit distinct isotopic signatures and elemental concentrations. We have now completed xenon isotopic analysis of each of the residues, including the light isotopes not previously measured.

About 1 µg of each grain size fraction was loaded directly onto separate Ta filaments and analysed by stepwise heating (about 15 steps) using the RELAX mass spectrometer [2]. Because of uncertainties regarding the amount of sample loaded onto each filament, our previously calculated Xe concentrations could not be confirmed in these analyses.

The new results (Fig. 1) confirm the systematic and significant differences in $^{136}\text{Xe}/^{132}\text{Xe}$ and $^{134}\text{Xe}/^{132}\text{Xe}$ ratios between the samples that we observed previously [1].

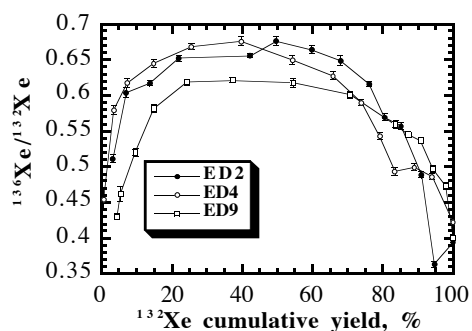


Fig. 1. Decreasing of the ratios at high temperatures is due to contribution of blank atmospheric Xe.

We have argued [1] that these variations in Xe isotopic composition are caused by different mixing ratios of Xe-HL and P3. Our new data add more details (Fig. 2). In particular there is some evidence of a small, but distinguishable, difference in the ratio of Xe-H to Xe-L for ED-4 (as revealed by comparing $\delta^{124}\text{Xe}$ and $\delta^{136}\text{Xe}$). ED-4 represents 6% of the total diamond separate, so this variation would not be apparent in bulk diamond analyses. We note even bigger effect in ED-4 observable as an apparent depletion in ^{126}Xe (Fig. 2). (We are currently attempting to confirm this depletion, which is present in several separate analyses). Furthermore, ED-9 (the largest grain size fraction) exhibits a slight but significant difference in its $^{134}\text{Xe}/^{136}\text{Xe}$ ratio compared to ED-2 and ED-4.

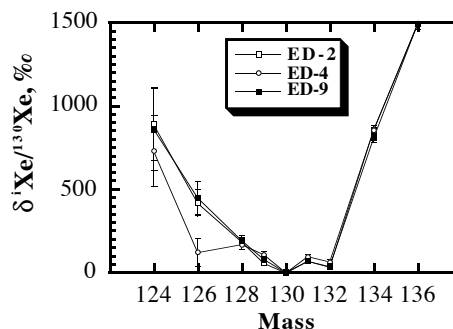


Fig. 2. Delta plots relative to BEOC-12 and scaled to $\delta^{136}\text{Xe}$ in the same fashion as [3]. For each sample the weighted average of several of the most representative steps were used.

The persistent inseparability of Xe-H from Xe-L has been a puzzling issue since the discovery of Xe-HL. It has been attributed to efficient mixing of diamonds in the solar nebula [4], while the effect of averaging during analysis may also be important since a few billion grains are necessary for Xe isotope measurements; diamonds appear to be destroyed at nearly the same temperature during stepwise analysis independent of grain size and other properties [5]. However, individual supernovae might be expected to produce distinctive grain size distributions and somewhat different isotopic signatures. It seems highly unlikely that mixing processes in individual supernovae would always produce the same xenon isotopic composition. Rather, we may expect different supernovae to show characteristic Xe-HL patterns. The diamond samples analysed here have been physically separated into grain size fractions that exhibit different isotopic signatures (including those for carbon [1]), so the search for variations in the Xe-H/Xe-L ratio becomes a critical test for astrophysical theories of origin of Xe-HL [e.g. 6]. Our preliminary results suggest that different supernovae appear to have different Xe-H/Xe-L ratios. We also speculate that the difference in $^{134}\text{Xe}/^{136}\text{Xe}$ between different grain size fractions may suggest some variations in the neutron fluence in the zone where Xe-H was formed in different supernovae [6].

References: [1] Verchovsky A. B. et al. (1998) *LPSC, XXIX*. [2] Gilmour J. D. et al. (1994) *Rev. Sci. Instrum.* 65, 617-625; [3] Nichols R.H. Jr. et al. (1991) *GCA*, 55, 2921-2936; [4] Howard W. M. et al. (1992) *Meteoritics*, 27, 404-412; [5] Huss G.R. and Lewis R.S. (1994) *Meteoritics* 29, 791-829; [6] Clayton D. D. (1989) *Ap. J.*, 340, 613-619

POLYTYPE VARIATIONS IN PRESOLAR SiC GRAINS: MICROSTRUCTURAL CHARACTERIZATION BY TRANSMISSION ELECTRON MICROSCOPY. T. L. Daulton¹, R. S. Lewis², and S. Amari³, ¹Argonne National Laboratory, Material Science Division, Argonne IL 60439-4838, ²Enrico Fermi Institute, University of Chicago, Chicago IL 60637-1433, ³McDonnell Center for the Space Sciences, Washington University, St. Louis MO 63130-4899.

Introduction: Microstructures produced during the formation of any material are highly dependent on both the conditions imposed during formation and the atomic-scale mechanisms of formation. Therefore, fossil microstructures of presolar grains archive valuable information concerning grain condensation mechanisms and the conditions within circumstellar grain forming regions.

An important component of presolar dust is SiC, which appears to contain several distinct grain populations. For example, Si- and C- isotopic compositions of the very largest SiC grains fall into several discrete clusters [1], while the isotopic compositions of trapped N show a grain size dependence [2].

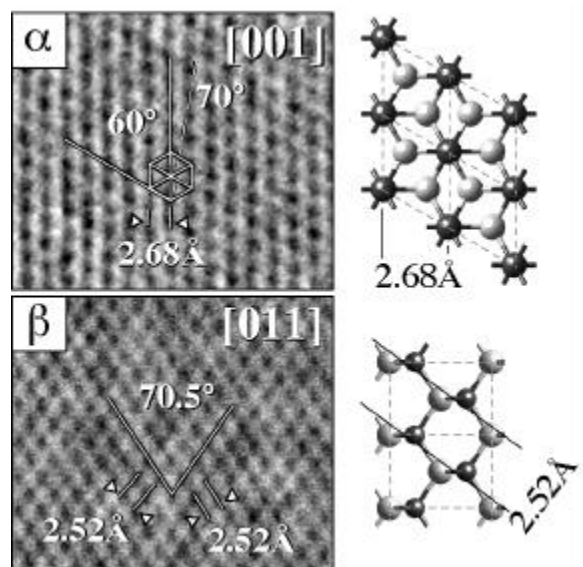
The crystallographic structure of SiC can adopt a range of polytype forms depending on the formation conditions. A characterization of the distribution of polytypes, stacking faults, twin planes, dislocations, phase intergrowths, and morphologies of presolar SiC can place constraints on their formation parameters. These parameters include the growth rates, temperatures, and pressures at which SiC grains condense from circumstellar outflows.

In this work, the microstructures of presolar SiC grains isolated by acid dissolution from the Murchison meteorite are studied by transmission electron microscopy. Preliminary results of this study are reported here.

Experiment: SiC isolated in the KJ series Murchison separates are distributed between 9 size fractions (KJA through KJI) [3]. Based on SEM measurements, 80% of the SiC grains are between 0.3-0.7 μm in diameter [3]. This corresponds to the size range in which greatest overlap between the nine size fractions occur. The KJB separate has been reported to contain the highest SiC abundance (1.91 ppm of the bulk meteorite), highest purity (97% SiC), and grain sizes characteristic of the total population (90% between 0.3-0.7 μm) [3].

In this work, the structure of ($\sim 0.3 \mu\text{m}$) SiC grains contained in KJB was identified by selected area diffraction and lattice imaging. A roughly equal abundance of the cubic (β) and hexagonal (α) polytypes were observed (c.f. Fig.). Recent C- and N- isotopic analysis of individual SiC grains (mean diameter 0.67 μm) in the KJC separate revealed they are predominantly presolar in origin [4]. A similar result was found for the SiC in the KJE separate [2]. Since the SiC populations in KJB-KJE overlap significantly, our TEM observations suggest that α -SiC is also a presolar dust component. This is in contrast to earlier work on individual large grains ($> 2 \mu\text{m}$) where every isotopically anomalous SiC grain, whose structure was identified by Raman spectroscopy, was cubic [1]. Since rapid growth has been shown to favor the cubic SiC polytype [5], the large, solely cubic SiC grains may have formed under different circumstellar conditions than those of α -SiC.

References: [1] Virag A. (1992), *GCA*, 56, 1715–1733. [2] Hoppe P. et al. (1996), *GCA*, 60, 883–907. [3] Amari S. et al. (1994) *GCA*, 58, 459–470. [4] Hoppe P. et al. (1998), 61st Met. Soc. Meeting. [5] Gmelin L. (1986) *Handbook of Inorganic Chem.*, Springer Verlag, p. 165.



Isotopic-ratio mapping using ion imaging has been very successful in locating rare types of presolar grains in meteoritic separates, *e. g.*, Al_2O_3 and Si_3N_4 [1–3]. This method has the advantage that large numbers of grains can be surveyed relatively quickly. However, it is limited both in which isotopic ratios can be analyzed and in the attainable precision. To avoid these limitations, we have developed a new system for fully automated isotopic-ratio measurements of micron-sized particles, using a Cameca IMS-6f ion microprobe. We have used this system to measure Si and C isotopes in ~ 250 presolar SiC grains from Murchison and identified members of rare sub-groups.

The new particle measurement system involves a number of steps. First, one or more images are acquired by rastering a small ($\sim 1\mu\text{m}$) primary beam over an area of the sample mount (~ 150 by $150\mu\text{m}$). Coordinates of different grains are obtained from the image(s) by image processing. Second, the primary ion beam is deflected to and centered on each grain in turn. A second set of deflectors re-centers the secondary ion beam in the mass spectrometer, maintaining high mass-resolution conditions even for large primary deflections. Third, each grain is analyzed for its isotopic composition. The measurement is stopped if a preset statistical precision is reached or if the secondary ion signal decays too rapidly indicating the grain is being sputtered away. Finally, once all the grains in an image have been analyzed, the sample stage is moved to a new position and the process is repeated. Mass peaks are centered periodically and the position of the ion beam is centered within the field aperture before each image acquisition. Initial tests on terrestrial standards indicate analytical uncertainties (based on the ranges observed in different standard grains) of about $\pm 10\%$ for Si and C, $\pm 17\%$ for O and $\pm 6\%$ for Mg (1σ). These values are 2–3 times individual measurement errors and are expected to be reduced with improvements to the system.

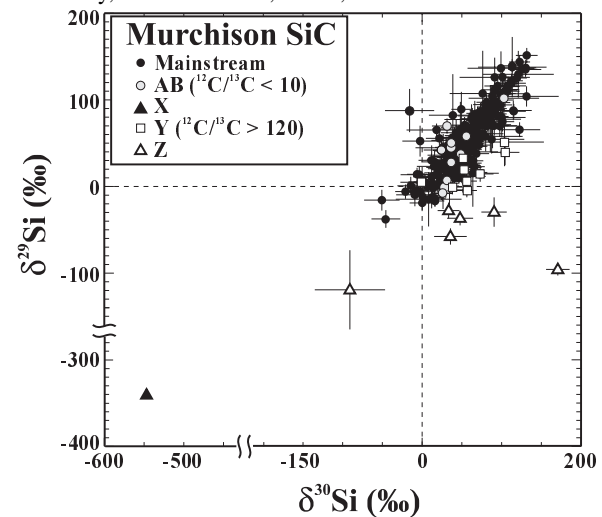
For this preliminary study, we have analyzed presolar SiC grains of nominal size $1\text{--}5\mu\text{m}$ from our Murchison separate [4]. A total of 339 grains were automatically located using ^{28}Si images and analyzed for their C- and Si-isotopic compositions. Of these ~ 250 had Si/C ratios indicative of SiC and analytical uncertainties less than $\pm 50\%$. The Si data for these grains are shown in the Figure. The distributions of Si and C isotopic ratios of these grains are in excellent agreement with previous observations of Murchison SiC [5]. Most of the grains lie along the “mainstream” line of slope 1.4 and members of

all the major sub-groups of presolar SiC were identified, as indicated in the Figure. Isotopic measurements of N, Al-Mg and Ti are planned for the largest grains of all types.

The efficiency of this new system at measuring grains depends primarily on the desired statistical precision of the measurements, the analyzed element(s), and the size of the grains. The data shown in the Figure were obtained in about one day, corresponding to 10–15 grains analyzed per hour. We anticipate that this could be increased up to ~ 50 grains/hour in some cases, for example mapping in $^{17}\text{O}/^{16}\text{O}$ and $^{18}\text{O}/^{16}\text{O}$ to search for presolar oxide grains.

Finally, we note that the routines developed here for automatically locating grains and centering them under the ion beam minimize the amount of time that grains are sputtered prior to being measured. This increases the amount of material available for analysis, which in turn allows smaller grains to be analyzed. Thus, the new system should be useful not only for locating *rare* types of presolar grains, but also for analyzing smaller members of *common* presolar grain populations.

References: [1] Nittler, L. R. *et al.*, *Nature* **370**, 443–446, 1994. [2] Nittler, L. R. *et al.*, *ApJ* **453**, L25–L28, 1995. [3] Hoppe, P. *et al.*, *Science* **272**, 1314–1316, 1996. [4] Alexander, C. M. O'D. *et al.*, *LPS XXIX*, Abstract # 1919, LPI, Houston, (CD-ROM), 1998. [5] Hoppe, P. and Ott, U., In *Astrophysical Implications of the Laboratory Study of Presolar Materials*, T. J. Bernatowicz and E. Zinner, eds., Woodbury, New York: AIP, 27–58, 1997.



DISTRIBUTION OF IN-SITU SILICON CARBIDE GRAINS IN PRIMITIVE METEORITES AND THEIR USE IN IDENTIFYING NEBULAR COMPONENTS. P. D. Swan and R. M. Walker, McDonnell Center for the Space Sciences, Washington University, St. Louis MO 63130 (rmw@howdy.wustl.edu).

We report the in-situ identification of 148 presolar SiCs in Murchison, Cold Bokkeveld, Acfer 094, and Orgueil. The mapping technique used to locate grains relies on the higher yield of Si x-ray photons, for a given electron current, for SiC than for other silicon bearing phases in the meteorite. The detection efficiency depends critically on the mapping conditions; in this work we used a Tracor Northern 5400 system operating at 10 keV with a standard 33 mm² Si-Li detector, Be window, a sample distance of 4.2 cm, a high amplifier setting to avoid pulse pileup, a magnification of 400x, a mapping array of 256 x 256 pixels, a beam current of 2 nanoamps and a dwell time of 0.01 sec per pixel. Under these conditions, the average counts in the Si channel (ROI - 1.67-1.81 keV) for a SiC standard is 120/pixel. All points in the image that satisfied the conditions Si > 43/pixel and Mg < 7/pixel, were remapped at higher magnification to verify the existence of Si "hotspots." Most of these corresponded to SiC grains as proved by the appearance of a C peak when a thin plastic window was substituted. Repeated mapping of known grains showed that the detection efficiency for locating SiC grains drops rapidly below a grain diameter of ~ 0.8 µm. A substantial number of O-rich grains of uncertain origin were also found. Contamination by terrestrial SiC is a problem. In our original work (1), we verified that grains were presolar by making ion probe measurements on them in the section itself. This was not feasible for the many grains reported here and their identification as indigenous is based on high magnification stereo images of each grain coupled with our judgments based on our previous experience in examining grains of known isotopic compositions. Care was also taken to avoid the use of SiC in the preparation of the samples, all of which were polished by Nat Saenz of Battelle Northwest (to whom we are deeply indebted) using an Al₂O₃ abrasive. The morphologies of the grains varied from rounded-blocky to elongate with no obvious differences noted between meteorites. Many grains appeared cracked suggesting that size distributions inferred from studies of SiC grains in acid residues should be viewed with caution. All save one of the SiCs occurred as rimless, isolated grains embedded in a fine-grained matrix. An exceptional grain in Acfer 094 was embedded in, or rimmed by, FeS. Some in situ grains were found in chondrule rims in both CM meteorites. This is consistent with the hypothesis that some rims consist of swept up nebular dust (2,3). Since circumstellar grains are the only meteoritic components that were certainly part of the protosolar

nebula, their presence can be used to test the nebular origin of rims and other meteorite constituents as, for example, a unique dark inclusion found in Ningqiang (4). The current slow rate at which in-situ grains are detected (0.5 to 1 grain per 24 hrs of mapping of Murchison) makes it difficult to obtain meaningful statistics for many applications. However, by the time of the conference, we hope to demonstrate a factor of 10 improvement in mapping speed, making it possible to measure circumstellar grains in different subunits in reasonable times.

References: [1] Alexander C. M. O'D. et al. (1990) *Nature*, 348, 715-717. [2] Cuzzi J. N. et al. (1998) *LPS*, Abstract #1439. [3] Metzler K. and Bischoff A. (1996) *Chondrules and the Protoplanetary Disk*, 153-161. [4] Zolensky et al. (1998) *LPS*, Abstract #1714.

PREDICTED SR, ZR, AND MO ISOTOPIC COMPOSITION IN PRESOLAR GRAINS FROM TYPE II SNE.

R. Gallino, *Dipartimento di Fisica Generale, Universita' di Torino, Via. P. Giuria 1, I-10125 Torino, ITALY, gallino@to.infn.it*, C. Travaglio, *Dipartimento di Astronomia e Scienze dello Spazio, Largo Fermi 5, I-50125 Florence, ITALY, claudiat@arcetri.astro.it*, E. Zinner, *McDonnell Center for the Space Sciences and the Physics Department, Washington University, One Brookings Drive, Saint Louis 63130, USA, ekz@howdy.wustl.edu*, S. Amari, *McDonnell Center for the Space Sciences and the Physics Department, Washington University, One Brookings Drive, S. Louis 63130, USA, sa@howdy.wustl.edu*, S. Woosley, *University of California Observatories/Lick Observatory, Board of Studies in Astronomy and Astrophysics, University of California, Santa Cruz, CA 95064, USA, woosley@lick.ucsc.edu*.

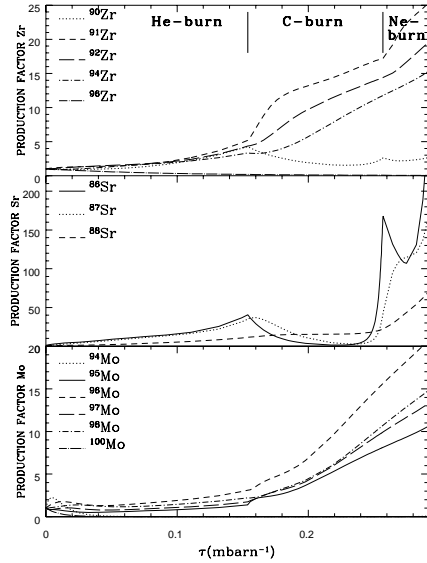


Figure 1: Isotopic abundances relative to solar versus accumulated neutron exposure during consecutive episodes of He-, C-, and Ne-burning for a $20 M_{\odot}$

Presolar Mainstream SiC grains show clear evidence of s -process Sr, Zr and Mo isotopic compositions [1,4], in agreement with what is inferred for the winds of AGB stars of low-mass and solar metallicity.

A different subclass of SiC grains, SiC-X, and low-density graphite grains from the Murchison CM2 chondrite, instead most likely condensed in the ejecta of SNe [5,6]. Since Zr and Mo carbide subgrains have been detected in presolar graphite grains [7], it is worth presenting predictions for the SN ejecta. The s -process occurring in massive stars under pre-explosive conditions is far different from the one occurring in low mass AGB stars. Massive stars are considered to be the source of the weak s -component in the solar system, accounting for s -isotopes from Fe up to Sr, whereas the AGB stars are the site of the main s -component, accounting for all s -isotopes beyond Sr. A very interesting feature is

shown by the Sr isotopes. Of the s -only isotopes $^{86,87}\text{Sr}$, only $\sim 50\%$ of their solar abundance derives from the weak s -component, and only a minor fraction of the neutron magic ^{88}Sr , while the p -only isotopes ^{84}Sr is destroyed by neutron capture in both sources. The production of $^{86,87}\text{Sr}$ is strongly affected by s -branching at ^{85}Kr , whose behavior depends on neutron density and temperature conditions. In particular, the isomeric state of ^{85}Kr has to be considered unthermalized during He burning in both AGB stars and in massive stars, while being fully thermalized during C-, Ne-, or O-burning conditions that occur in massive stars. A second key point is the completely different nature of neutron captures in AGB stars and in massive stars. In low-mass AGB stars, the major source of neutrons is provided by the ^{13}C source, the alternative ^{22}Ne source playing only a minor role.

In contrast, ^{22}Ne is the major neutron source in massive stars. Eventually, in the inner O-burning shell conditions occurring almost explosively, also the reaction $^{26}\text{Mg}(\alpha, n)^{29}\text{Si}$ plays an important role. Moreover, the s -process yields in the various zones of supernova ejecta are a combination of different neutron capture histories. Differences for the Zr and Mo isotopes are expected due to the treatment of s -branching occurring at ^{89}Sr and ^{90}Y , two channels partially open under high neutron density conditions implied by C- and Ne-burning in massive stars, and at ^{95}Zr , which is sensitive to lower neutron densities.

Fig. 1a,b,c shows the predicted Sr, Zr, and Mo isotopic production factors normalized to solar obtained with an updated s -process code in a $20 M_{\odot}$ star during He-burning, followed by convective shell C- and Ne-burning. The different behaviour of isotopes dependent on s -branching is apparent. Some interesting features can be sketched. ^{90}Zr is marginally produced under all conditions, and ^{96}Zr is underproduced, while the other Zr isotopes are relatively enhanced. This is a quite different behaviour from what is expected in AGB stars, where ^{96}Zr is fed in the late AGB phases. The most important feature for Sr is the relatively low ^{88}Sr yield with respect to $^{86,87}\text{Sr}$, which is just the reverse of what happens in AGB stars. A slightly different behaviour

can be discerned in the Mo isotopes. Mixing exercises of SN ejecta are in progress. They will also consider the important yields derived in the inner Si-rich region adjacent to the Ni core as obtained with a full network during the implosion of the O-rich inner layers built in hydrostatic conditions, followed by the final explosion [8].

REFERENCES

- [1] Ott U. & Begemann F. (1990), *Lunar Planet. Sci.* XXI, 920 [2] Podosek, F. et al. (1998), *ApJ*, in press.
- [3] Nicolussi, G. K. et al. (1997), *Science*, 277, 1281. [4] Nicolussi, G. K. et al. (1998), *GCA*, submitted. [5] Travaglio, C. et al. (1998) *Astrophys. J.*, submitted. [6] Zinner, E. et al. (1998) *LPS* 29, Abstract 1763. [3] Woosley, S.E. and Weaver, T.A. (1995) *Astrophys. J. Suppl.* 101,181. [7] Bernatowicz, T.J. and Cowsik, R. (1997), *Astrophysical Implications of the Laboratory Study of Presolar Materials*, ed. T. Bernatowicz & E. Zinner, (New York: AIP), 451. [8] Woosley, S.E. and Weaver, T.A. (1998), unpublished

PRESOLAR GRAINS FROM SN TYPE II: THE CASE OF THEIR SI AND CA ISOTOPIC COMPOSITIONS. C. Travaglio, *Dipartimento di Astronomia e Scienze dello Spazio, Largo Fermi 5, I-50125 Florence, ITALY, claudiat@arcetri.astro.it*, R. Gallino, *Dipartimento di Fisica Generale, Universita' di Torino, Via. P. Giuria 1, I-10125 Torino, Italy, gallino@to.infn.it*, E. Zinner, *McDonnell Center for the Space Sciences and the Physics Department, Washington University, One Brookings Drive, St. Louis 63130, USA, ekz@howdy.wustl.edu*, S. Amari, *McDonnell Center for the Space Sciences and the Physics Department, Washington University, One Brookings Drive, St. Louis 63130, USA, sa@howdy.wustl.edu*, S. Woosley, *University of California Observatories/Lick Observatory, Board of Studies in Astronomy and Astrophysics, University of California, Santa Cruz, CA 95064, USA, woosley@lick.ucsc.edu*.

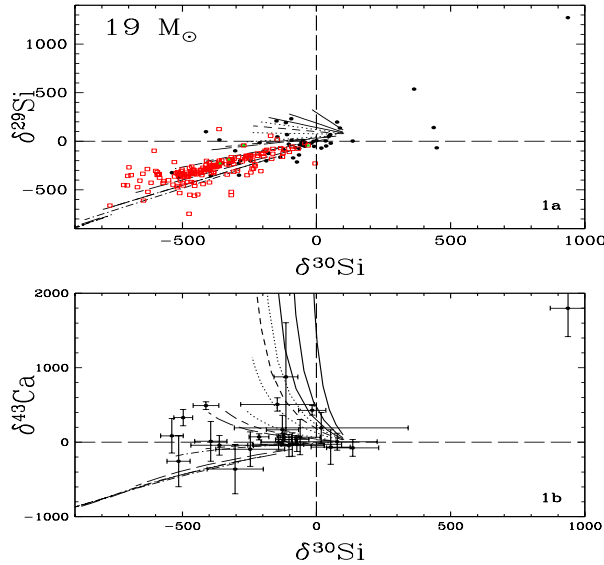


Figure 1: Predicted isotopic compositions in ejecta from a $19 M_{\odot}$ SN as compared with those of presolar SN grains.

Low density graphite grains, a subset of SiC grains (SiC-X), and a handful of nitride grains extracted from the Murchison carbonaceous chondrite exhibit isotopic compositions indicative of their origin in supernova ejecta. If their Si isotopic compositions are compared with the results of a series of mixing exercises in SN ejecta [1,2], based on SN models of the various nucleosynthetic zones [3], there is a clear indication of a deficiency of $^{29}\text{Si}/^{28}\text{Si}$ in the predicted SN yields by about a factor of two. A similar observation was reported by [4]. The discrepancy can be overcome by increasing the ^{29}Si yield in the

O-rich region that suffered shell Ne-burning. The nucleosynthesis yields of the SN models [3] were obtained using the estimated rate of the reaction $^{26}\text{Mg}(\alpha, n)^{29}\text{Si}$ by [5]. An analysis of the various reaction rates playing a role led us to infer that a convenient solution may be obtained by roughly doubling the above rate. The results of various mixing tests is shown in Fig. 1a for a $19 M_{\odot}$ SN model, after doubling the rate in a post-processing simulation. Experimental efforts to improve the accuracy of this reaction rate have been envisaged [6]. This modification of the rate may also solve the more fundamental problem, already stressed by [7], that SN models [3 and 8] for a large range of stellar masses do not produce ^{29}Si and ^{30}Si in the cosmic ratio 1.7, but with approximately equal abundances [9]. The consequences of a rate change would also affect the much debated problem of the Si isotopic composition in mainstream presolar SiC grains [e.g. 7].

The $19 M_{\odot}$ SN model appears capable of reproducing other measured isotopic ratios in SN grains. In Fig 1b predicted $\delta(^{43}\text{Ca})$ versus $\delta(^{30}\text{Si})$ are compared with existing measurements in single grains.

REFERENCES

- [1] Travaglio, C. et al. (1998) *Astrophys. J.*, submitted.
- [2] Zinner, E. et al. (1998) *LPS 29*, Abstract 1763.
- [3] Woosley, S.E. and Weaver, T.A. (1995) *Astrophys. J. Suppl.* 101,181.
- [4] Nittler, L.R. et al. (1995) *Astrophys. J.* 453, L25.
- [5] Caughlan, B. and Fowler, W.A. (1985), *Atom. Data Nucl. Data Tabl.*, 40, 283
- [6] Denker, A. et al. (1985), in *Nuclei in the Cosmos III*, ed. M. Busso, R. Gallino, and C.M. Raiteri, New York: AIP, 255
- [7] Timmes, F.X. and Clayton, D.D. (1996) *Astrophys. J.* 472, 723.
- [8] Thielemann, F.-K. et al. (1996), *Astrophys. J.* 460, 408.
- [9] Timmes, F.X., Woosley, S.E., Weaver, T.A. (1995) *Astrophys. J. Suppl.* 98,617.

STRONTIUM ISOTOPES IN SINGLE PRESOLAR SiC GRAINS. G. K. Nicolussi^{1,2}, M. J. Pellin¹, R. S. Lewis², A. M. Davis², R. N. Clayton^{2,3,4}, and S. Amari⁵, ¹Materials Science and Chemistry Division, Argonne National Laboratory, Argonne IL 60439, USA, ²Enrico Fermi Institute, ³Department of Chemistry, ⁴Department of the Geophysical Sciences, The University of Chicago, Chicago IL 60637, USA, ⁵McDonnell Center for Space Sciences, Washington University, St. Louis MO 63130, USA.

Eleven individual SiC grains from the Murchison meteorite were analyzed for their Sr isotopic compositions by laser ablation combined with resonant ionization mass spectrometry. The majority of the analyzed grains have $^{87}\text{Sr}/^{86}\text{Sr}$ and $^{88}\text{Sr}/^{86}\text{Sr}$ ratios which are normal within the experimental uncertainties. However, large deficits were found for the p -isotope ^{84}Sr . The Sr isotopic data found for these 11 grains are consistent with the s -process at low neutron densities in which the nucleosynthesis of Sr is affected by β decay of short-lived ^{85}Kr ($T_{1/2} \sim 10.8$ a).

Introduction: Circumstellar dust grains found in a variety of primitive meteorites condensed from stellar outflows or from stellar explosion ejecta and provide important constraints on nucleosynthesis theory [1]. Most presolar SiC grains isolated from these meteorites have light element isotopic compositions consistent with formation around AGB stars [2]. In previous analyses we have measured isotopic abundances of Zr and Mo in presolar SiC [3,4]. The large and variable s -process enrichments in Zr and Mo seen in “mainstream” SiC are also entirely consistent with grain formation in the H-envelope of AGB stars. Sr measurements on aggregates of Murchison SiC grains have shown large negative $\delta^{84}\text{Sr}/^{86}\text{Sr}$ values but very small variations in $\delta^{87}\text{Sr}/^{86}\text{Sr}$ and $\delta^{88}\text{Sr}/^{86}\text{Sr}$ [5].

Experimental: The Sr isotopic composition was measured on the CHARISMA instrument by using resonant ionization mass spectrometry in order to selectively ionize and detect the Sr isotopes [3,4,6]. The SiC grains used here are from the Murchison KJG fraction with a typical grain size of $\sim 2\text{--}4$ μm in diameter. Prior to isotopic analysis, the SiC grains were mapped with a scanning electron microscope.

Results and Discussion: Sr has four stable isotopes. ^{84}Sr is a p -process isotope which is shielded from the s - and r -processes. ^{86}Sr is a pure s -process isotope, shielded from the r -process by ^{86}Kr . ^{87}Sr is also an s -process isotope; however, it can be produced by decay of ^{87}Rb ($T_{1/2} \sim 48$ Ga). ^{88}Sr is mainly an s -process isotope but it has some r -process contributions in its terrestrial composition. In Fig. 1 the results for 11 individual SiC grains are shown in form of three-isotope plots in which ^{86}Sr was used for normalization. Generally, very large deficits in the abundance of the p -isotope ^{84}Sr were found which is consistent with s -process nucleosynthesis [7]. The solar-like $^{87}\text{Sr}/^{86}\text{Sr}$ reflects that their ratio depends only on the relative neutron capture cross sections. Synthesis of ^{86}Sr and

^{87}Sr requires that the s -process path runs from ^{84}Kr to ^{85}Rb to ^{86}Sr via the unstable nuclei ^{85}Kr and ^{86}Rb . Because of the predominant β decay at the ^{85}Kr branch an upper limit for the neutron density at the s -process site can be inferred [8]. Decay of ^{87}Rb contributes very little to the ^{87}Sr abundance in the SiC grains. Two grains have significantly enhanced $^{88}\text{Sr}/^{86}\text{Sr}$ ratios and very low $^{84}\text{Sr}/^{86}\text{Sr}$ ratios. This indicates neutron capture on ^{85}Kr which bypasses the synthesis of ^{86}Sr and ^{87}Sr but would produce ^{88}Sr . Generally, the $^{88}\text{Sr}/^{86}\text{Sr}$ ratios show a much larger spread compared to analyses on SiC aggregates [5].

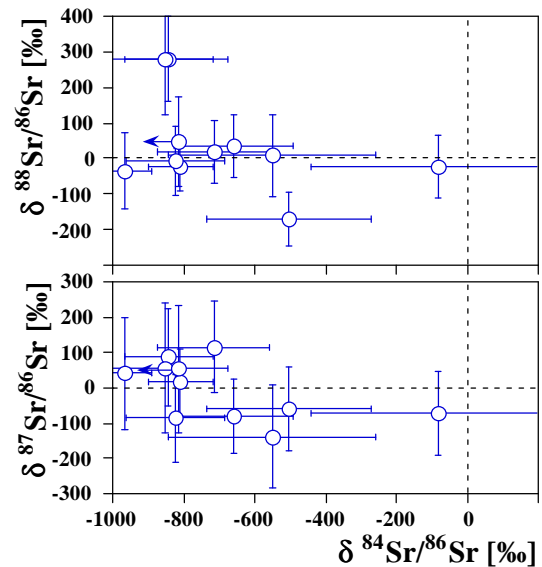


Fig. 1. Three-isotope plots of Sr from 11 individual SiC grains (error bars $\pm 2\sigma$)

Acknowledgments: This work was supported by the U.S. DOE, BES-Materials Sciences, under Contract W-31-109-ENG-38 and by NASA Grants NAG5-3986, NAG5-4297, and NAG5-4298.

References: [1] Bernatowicz T. J. and Zinner E. (eds.) (1997) *Astrophysical Implications of the Laboratory Study of Presolar Materials*. AIP Press. [2] Hoppe P. et al. (1994) *ApJ*, 430, 870. [3] Nicolussi G. K. et al. (1997) *Science*, 277, 1281. [4] Nicolussi G. K. et al. (1998) *GCA*, 62, in press. [5] Podosek F. A. et al. (1998) *ApJ*, in press. [6] Nicolussi G. K. et al. (1997) *Anal. Chem.*, 69, 1140. [7] Gallino R. et al. (1997), in ref. [1], 115. [8] Lambert D. L. et al. (1995) *ApJ*, 450, 302.

CARBON AND NITROGEN ISOTOPIC COMPOSITIONS OF INDIVIDUAL, SUBMICROMETER-SIZED PRESOLAR SILICON CARBIDE GRAINS. P. Hoppe^{1,2}, Th. Kocher², P. Eberhardt², S. Amari^{3,4}, and R. S. Lewis⁴, ¹Max-Planck-Institute for Chemistry, P.O. Box 3060, D-55020 Mainz, Germany, ²Physikalisches Institut, University of Bern, CH-3012 Bern, Switzerland, ³McDonnell Center for the Space Sciences, Washington University, St. Louis MO 63130-4899, USA, ⁴Enrico Fermi Institute, University of Chicago, Chicago IL 60637-1433, USA.

To date, most information on the isotopic compositions of individual presolar SiC grains has been obtained for grains with sizes $>1\ \mu\text{m}$ [e.g., 1-4]. While the isotopic compositions of the major elements C and Si do not show a clear dependency on grain size, the typical $^{14}\text{N}/^{15}\text{N}$ ratio was observed to increase with decreasing grain size [3]. Variations of isotopic compositions with grain size are also evident for Kr and Ba measured in SiC bulk samples [5,6]. As most of the mass of presolar SiC is in grains with sizes $<1\ \mu\text{m}$ [7, 8] a characterization of the isotopic properties of such grains is important in order to get a complete picture on the origin of presolar SiC grains found in primitive meteorites.

Here we report the results of C- and N-isotopic analyses made on 211 individual SiC grains from the Murchison separate KJC, having an average grain size of $0.67\ \mu\text{m}$ [7]. Similar to the larger grains, most KJC grains are characterized by enrichments in ^{13}C and ^{14}N relative to the solar abundances ($^{12}\text{C}/^{13}\text{C} = 89$, $^{14}\text{N}/^{15}\text{N} = 272$). The $^{12}\text{C}/^{13}\text{C}$ ratios range from 4.5 to 290 (median 51), and $^{14}\text{N}/^{15}\text{N}$ ratios are between 7 and 17000 (median 1400). About 90% of the grains belong to the group of the Mainstream grains [2] believed to have formed in the atmosphere of AGB stars. No type A grains ($^{12}\text{C}/^{13}\text{C} < 3.5$ [2]) are observed among the KJC grains. In the larger grain size separates, such grains make up about 2% of the total SiC. The origin of the type A grains is still controversial. The absence of such grains in the KJC sample of this study might be a hint that the type A grains formed in stellar environments that favor the growth of relatively larger grains. The observed correlation between the typical $^{14}\text{N}/^{15}\text{N}$ ratio, and the grain size does not extend to the smaller KJC grains. However, the N contents of single KJC grains are only at the femtogram level and are susceptible to terrestrial N contamination. We can thus not exclude that the intrinsic $^{14}\text{N}/^{15}\text{N}$ ratios of the KJC grains are higher than those measured.

About 1% of the SiC grains from the larger grain size separates are of type X, believed to have formed in the ejecta of Type II Supernova explosions [9]. From the C and N data we estimate the X grain abundance in the KJC separate to be about 1–1.5%. This number is supported by the identification of 21 X grains by Si ion imaging of ≈ 2000 KJC grains [10]. It is remarkable that the X-to-Mainstream grain abundance ratio is apparently independent of grain size, at least in the size range $0.5\text{--}5\ \mu\text{m}$. This might be a hint that the grain size distributions of SiC from AGB stars and Type II Supernovae are very similar.

This work was supported by the Schweizerischer Nationalfonds and by NASA.

References: [1] Alexander C. M. O'D (1993) *GCA*, 57, 2869. [2] Hoppe P. et al. (1994) *ApJ*, 430, 870. [3] Hoppe P. et al. (1996) *GCA*, 60, 883. [4] Huss G. R. et al. (1997) *GCA*, 61, 5117. [5] Lewis R. S. et al. (1990) *Nature*, 348, 293. [6] Prombo C. A. (1993) *ApJ*, 410, 393. [7] Amari S. et al. (1994) *GCA*, 58, 459. [8] Russell S. S. et al. (1997) *Meteoritics Planet. Sci.*, 32, 719. [9] Amari S. et al. (1992) *ApJ*, 394, L43. [10] Hoppe P. et al. (1996) *Meteoritics Planet. Sci.*, 31, A64.

NITROGEN-15-RICH NITROGEN IN METEORITES: POLYMICT UREILITES AND BENCUBBIN. G. P. Rooke, I. A. Franchi, A. B. Verchovsky, and C. T. Pillinger, Planetary Sciences Research Institute, Open University, Milton Keynes, MK7 6AA, UK (g.p.rooke@open.ac.uk).

Most meteorites have whole-rock N $\delta^{15}\text{N}$ from -90‰ to +100‰. A small group contain N with much larger $\delta^{15}\text{N}$ values: some even reaching +1000‰ or higher: Bencubbin, Acfer 182, CR chondrites and polymict ureilites. This study is aimed at determining the origin of this heavy N. The approach is to attempt to concentrate any carriers of the N component and establish if any other distinct isotopic signatures are associated with the N. This would help determine the possible mechanism for generating the ^{15}N enrichment. Samples (whole-rock and acid residues) were stepped heated and the ^4He , $^{12,13}\text{C}$, $^{20,21,22}\text{Ne}$ and $^{36,38,40}\text{Ar}$ together with N analysed on the automated mass spectrometer system, FINESSE.

Initial investigations concerned Bencubbin, a stony iron breccia with unique clasts shock welded into a glassy matrix and a whole-rock N isotopic composition of $\delta^{15}\text{N} \approx 1000\text{‰}$ [1]. Despite a previous extensive study [2] the origin of the heavy N has remained elusive. This study showed that virtually all the heavy N is located in an acid resistant phase (combustion temperature $\approx 400^\circ\text{C}$) shielded by a refractory but acid soluble phase. A conjoint noble gas, C and N analysis of acid residues suggested a possible association between the heavy N carrier and a small amount of planetary argon, however it was understood that this could be an effect of acid damage to the main argon carrier [3,4].

To eliminate the possible acid damage to the argon carrier (and N carrier), a much milder treatment with CuCl_2 was devised [5,6]. This resulted in the removal of Fe-Ni metal from the clasts and matrix leaving the sulphide and silicate clasts and silicate glass. Analysis of the residues from this treatment established that there was no association between the acid resistant phase containing the heavy N and any detectable noble gas or C release, indicating that the heavy N carrier in Bencubbin is isolated from noble gases and C.

More recently investigations have been extended to polymict ureilites. This has also entailed a survey of

main group ureilites (MGUs) to enable resolution of features unique to polymict ureilites. Two MGUs (ALHA 77257, HH126) and three polymict ureilites (Nilpena, EET 87720, North Haig) have been investigated [7]. All the ureilite release profiles were dominated by the release of isotopically light N, C and planetary noble gases at $\approx 600^\circ\text{C}$, a cosmogenic neon release at $\approx 750^\circ\text{C}$ and a low temperature release of N at $\approx 300^\circ\text{C}$ with an isotopic composition of $\delta^{15}\text{N} \approx 20\text{‰}$. In the polymict ureilites, the N composition became much heavier between 300°C and 600°C , up to $\delta^{15}\text{N} \approx 120\text{‰}$, but without any detectable peak in the release profile. This indicates that a relatively small amount of isotopically heavy N is being released on the shoulder of the isotopically more "normal" N. More importantly, as with Bencubbin, the heavy N release does not appear to be associated with any noble gas or C release.

The isolation of the heavy N carrier from noble gases in the polymict ureilites and Bencubbin seems to indicate that the N is chemically bound to a carrier and rules out a cosmogenic origin for the heavy N. There being no other unusual signatures makes a pre-solar grain origin also unlikely. This leaves some form of extreme isotopic fractionation as the most viable remaining possibility. A common link with all these meteorites is the brecciation event. This could suggest that the N carrier is a late stage nebular residue component which may have been carried into the regolith gravitationally or with the impactor.

References: [1] Prombo C. A. and Clayton R. N. (1985) *Science*, 230, 935–937. [2] Franchi I. A. et al (1986) *Nature*, 323, 138–140. [3] Rooke G. P. et al (1996) *Meteoritics*, 31, 4 Supp, A118. [4] Rooke G. P. et al. (1996) *59th Meteoritical Society Meeting*, Poster Presentation. [5] Rooke G. P. et al (1997) *LPS XXVIII*, 1195–1196. [6] Rooke G. P. et al (1997) *LPS XXVIII*. [7] Rooke G. P. et al (1998) *LPS XXIX*, #1744.

THE "21-MICROMETER" INFRARED FEATURE IN BULK DIAMONDS: IMPLICATIONS FOR NANODIAMONDS IN SPACE. H. G. M. Hill^{1,2}, A. P. Jones², and L. B. d'Hendecourt², ¹Muséum National d'Histoire Naturelle, 61 Rue Buffon, 75005 Paris, France, ²Institut d'Astrophysique Spatiale (CNRS), Université Paris XI - Bâtiment. 121, 91405 Orsay Cedex, France.

It is often said that "no two diamonds are alike." This is because the lattice structure of *all* diamonds is defective to some degree and in a singular way. Such defects include substituted elements, vacancies, disorder, etc., which can modify the thermal, mechanical, and optical properties of diamond. For example, N in its various substitutional forms, can destroy the translational symmetry of the "perfect" diamond lattice and activate first-order infrared (IR) modes at $\lambda > 7.5 \mu\text{m}$ which are otherwise forbidden in bulk 3C cubic material [1]. It is our contention that meteoritic nanodiamonds *also* have defect-activated (one-phonon) IR features as they possess "defective" surfaces and lattices [2-4]. However, it is extremely difficult to search for weak, intrinsic absorption features in meteoritic nanodiamond residue on account of: (1) dominant, artefact-related features, (2) limited quantities of this material available for spectral analysis, and (3) the relative weakness of *all* IR features in diamond. Therefore, we have analysed a "defective," N-rich (Type IaA) bulk diamond and also a "perfect," N-poor (Type IIa) bulk diamond irradiated with fast neutrons (fluence: 3.1×10^{18} neutrons cm^{-2}) to introduce lattice defects (Fig. 1a-c). The IR spectrum of the "N-poor" diamond is greatly modified at $\lambda > 7.5 \mu\text{m}$ following neutron irradiation with new features appearing at 8.3, 9.1, 10.0 and 22.0 μm in the one-phonon region (Fig. 1b,c). These features are similar to those of the "N-rich" diamond (Fig. 1a). Most, or all, of these features are caused by symmetry-breaking and the activation of ("forbidden") first-order IR modes [1]. We suggest that 'imperfect' nanodiamonds also have similar, active, one-phonon bands [3]. *The ~21 μm feature is common to both the "N-rich" and irradiated "N-poor" diamonds* (Fig. 1a,c) and is not due to a contaminant. Its precise origin is unknown but it could be due to a, hitherto unreported, "molecular-type" vibration associated with lattice defects such as those created by N impurities or neutron irradiation. We submit that this feature is common in defective bulk diamonds and also in nanodiamonds and, hence, reiterate [3,4] that nanodiamonds are possible carriers of the 21 μm unidentified infrared feature seen in emission around some C-rich, protoplanetary nebulae (PPNe). Indeed, we have recently calculated the emission spectrum for Type IaA diamond (using data from Fig. 1a) and found an excellent fit with PPNe spectra for the IRAS sources 07134+1005, 22272+5435 and

23304+6147, for emission temperatures of the order of 150–200 K. These dust temperatures are typical of PPNe dust shells and further suggest that the 21- μm band in these sources may be due to emission from nanodiamonds.

Acknowledgements: We thank J. W. Harris and DeBeers for the loan of the Type IaA diamond and Laboratoire Pierre Süe, Saclay, for performing the neutron irradiation experiment.

References: [1] Smith S. D. and Hardy J. R. (1960) *Philosophical Mag.*, 5, 1311–1314. [2] Bernatowitz T. J. et al. (1990) *Astrophys. J.*, 359, 246–255. [3] Hill H. G. M. et al. (1997) *Meteoritics & Planet. Sci.*, 32, 713–718. [4] Hill H. G. M. et al. (1998) *Astron. Astrophys.*, (in press).

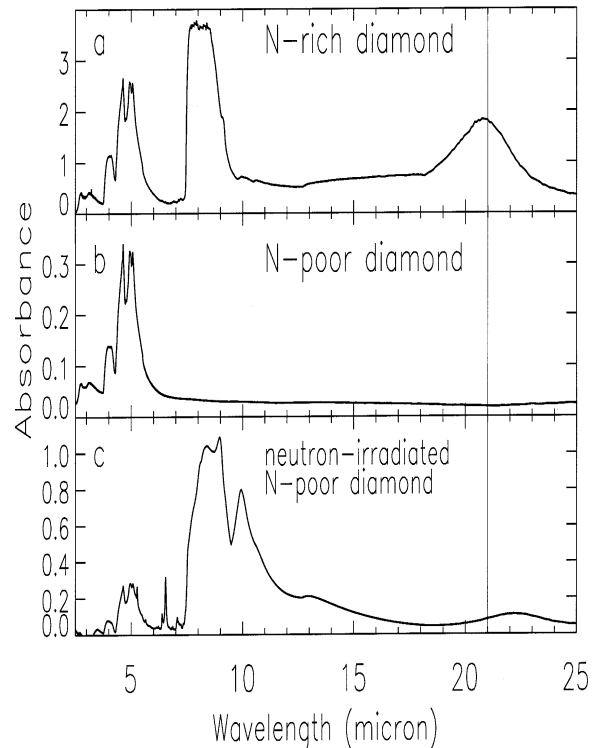


Fig. 1. Mid-IR spectra of bulk diamonds: (a) "N-rich" Type IaA, (b) "N-poor" Type IIa, and (c) "N-poor" Type IIa after irradiation with fast neutrons. Vertical line marks 21- μm wavelength position.